Food Bioscience 56 (2023) 103106

Contents lists available at ScienceDirect

Food Bioscience

journal homepage: www.elsevier.com/locate/fbio

Iron-peptide complexes from spent yeast: Evaluation of iron absorption using a Caco-2 monolayer

Ana Sofia Oliveira [a], Carlos M.H. Ferreira [a,b,**], Joana Odila Pereira [a,b,***], Sara Silva [a], Eduardo M. Costa [a], Ana Margarida Pereira [a,b], Margarida Faustino [a], Joana Durão [a,b], Manuela E. Pintado [a], Ana P. Carvalho [a,*]

[a] *Universidade Católica Portuguesa, CBQF - Centro de Biotecnologia e Química Fina – Laboratório Associado, Escola Superior de Biotecnologia, Rua Diogo Botelho 1327, 4169-005, Porto, Portugal*

[b] *Amyris Bio Products Portugal Unipessoal Lda, Rua Diogo Botelho 1327, 4169-005, Porto, Portugal*

A R T I C L E I N F O

Keywords:
Iron uptake
Iron bisglycinate
Ferritin
Iron bioavailability
Saccharomyces cerevisiae

A B S T R A C T

Anaemia is one of the most prevalent nutritional diseases worldwide with Fe deficiency being its major cause. In fact, the limited bioavailability of dietary iron and its interaction with food compounds contribute to its poor absorption in the human body and dietary Fe supplementation has been widely used to address this issue. By incorporating a circular economy framework, this study takes a novel approach of production of iron-peptide complexes from spent yeast peptide-rich extracts as a more effective substitute to conventional salt-based iron supplements, which are related with adverse consequences. Considering the regulation of iron absorption on duodenal enterocytes, iron-peptides complexes absorption was assessed using a Caco-2 monolayer, evaluating both iron uptake and the capacity to stimulate ferritin synthesis, after their *in vitro* simulated gastrointestinal digestion following INFOGEST protocol. An iron salt and a commercially available benchmark (iron bisglycinate) were also included in this study to compare the absorption performance. Results showed that iron-peptide complexes exhibited a similar behaviour (no statistically significant alterations ($p > 0.05$)) concerning the other tested samples, thus being a promising alternative for iron dietary supplementation. The remaining digested peptides from the complexes also showed potential antioxidant activity, suggesting protection of iron from oxidation within human body.

1. Introduction

Fe is an important micronutrient for human health since it is involved in several essential metabolic pathways such as oxygen transport, oxidative phosphorylation, synthesis and use of porphyrin, and regulation of the immune system, among other functions (Jeppsen & Borzelleca, 1999). Since adults may lose up to 2 mg of Fe *per* day by tissue shedding and through the digestive tract, Fe needs to be ingested through diet in quantities that allow for the maintenance of its optimum levels. Dietary intake of Fe includes two forms which are differently absorbed by the human body: heme and non-heme Fe (elemental Fe). Both are mostly absorbed in the first portion of the intestine, namely duodenum and proximal jejunum, by differentiated enterocytes geared for vectorial transport of Fe and other nutrients. In fact, Fe movement may be divided into three main steps: 1) Fe entrance in the enterocyte; 2) movement of Fe inside the cell to the basal layer and 3) export of Fe from the enterocyte through the basal layer into circulation (Collins & Anderson, 2012). Heme Fe is present mainly in meat, poultry and fish, being ready to be absorbed by the folate transporter present in duodenal enterocytes. On the other hand, elemental Fe absorption, found in plant foods in two valence states (Fe^{2+} or Fe^{3+}), may be affected by different factors related to gastrointestinal tract (GIT): enzymes, pH and

* Corresponding author. Universidade Católica Portuguesa, CBQF - Centro de Biotecnologia e Química Fina – Laboratório Associado, Escola Superior de Biotecnologia, Rua Diogo Botelho 1327, 4169-005, Porto, Portugal.

** Corresponding author. Universidade Católica Portuguesa, CBQF - Centro de Biotecnologia e Química Fina – Laboratório Associado, Escola Superior de Biotecnologia, Rua Diogo Botelho 1327, 4169-005, Porto, Portugal.

*** Corresponding author. Universidade Católica Portuguesa, CBQF - Centro de Biotecnologia e Química Fina – Laboratório Associado, Escola Superior de Biotecnologia, Rua Diogo Botelho 1327, 4169-005, Porto, Portugal.

E-mail addresses: chferreira@ucp.pt (C.M.H. Ferreira), jodila@ucp.pt (J.O. Pereira), apcarvalho@ucp.pt (A.P. Carvalho).

https://doi.org/10.1016/j.fbio.2023.103106
Received 8 June 2023; Received in revised form 17 July 2023; Accepted 4 September 2023
Available online 6 September 2023

interactions with other food components (phytates, oxalates and polyphenols) (Anderson, Lu, Frazer, & Collins, 2018; Collins & Anderson, 2012; Shubham et al., 2020). To be absorbed by the duodenal enterocytes, elemental Fe needs to be reduced to its ferrous form (Fe^{2+}) by reducing agents, such as duodenal cytochrome *b*, so it can be later transported by divalent metal transporter 1 (DMT1) into the duodenal cytoplasm. Both valence Fe states (Fe^{2+} and Fe^{3+}) are present in the apical layer of the enterocyte where the Fe pathway starts (Anderson et al., 2018; Collins & Anderson, 2012; Wu, Yang, Sun, Bao, & Lin, 2020).

Besides the challenge of non-heme Fe absorption, the amount of bioavailable dietary Fe is considered low (5–18%) (Eckert et al., 2016), thus contributing to human Fe deficiency, which is the major cause of one of the most prevalent nutritional diseases worldwide - anaemia (Wu, Li, Hou, Zhang, & Zhao, 2017). Indeed, the World Health Organization (WHO) estimates that 1.62 billion people are globally affected by this disease (World Health Organization, 2008), highlighting the prevalence numbers of 30% for women (15–49 years) and 40% for children (<5 years) in 2019 (World Health Organization, 2021). To address this issue, Fe food fortification has been used worldwide by applying Fe salts, namely sulphate, carbonate, citrate, and fumarate, despite their low bioavailability. This implies the use of a high quantity of salts for Fe levels correction, which causes health problems such as gastrointestinal irritations, among many others. Additionally, these Fe salts may interact with food components provoking flavour, texture and colour changes (Athira, Mann, Sharma, Pothuraju, & Bajaj, 2021; Caetano-Silva, Bertoldo-Pacheco, Paes-Leme, & Netto, 2015; Shubham et al., 2020).

As an alternative to conventional salt-based Fe supplementation, proteins and peptides have been applied in the production of Fe complexes (Athira et al., 2021). These molecules are capable of binding Fe through their amino acid sequences by electrostatic interactions and coordinate bonding, keeping it soluble. Since Fe-peptide complexes may improve Fe solubility, they can increase its uptake and transport in duodenal enterocytes (Caetano-Silva et al., 2015).

Currently, one of the main non-animal protein and peptide sources used in the food industry is spent yeast, particularly *Saccharomyces cerevisiae*. A dry weight basis of up to 60% protein, the identification as a "Generally Recognized as Safe" (GRAS) microorganism, and the rising availability of this by-product (due to the growth of the brewing industry, about 2–4 kg of spent yeast *per* 100 L of beer produced) are the main reasons for the enhanced use (Oliveira, Ferreira, Pereira, Pintado, & Carvalho, 2022a). Moreover, the growth of other industries that use fermentation processes, such as synthetic biology, starts to contribute for the increase of engineered spent yeast that can also be valued in a circular economy approach (Oliveira et al., 2022c). In previous studies, authors have demonstrated that a peptide-rich extract with bioactivity properties could be attained from the liquid waste streams that result from β-glucan extraction from engineered spent yeast, using membrane separation technology (Oliveira et al., 2022d). This fraction was successfully complexed with Fe to produce Fe-peptide complexes (Ferreira et al., 2022; Oliveira et al., 2023).

Once Fe-peptide complexes pass intact through the GIT and Fe is released from them at the duodenum, minerals and peptides may follow their usual route for absorption in different pathways. Bioactive peptides may enter the cells through specific peptide transporters present in the intestinal epithelium, such as peptide transporter (PepT1) for di- and tripeptides, endocytosis of the cell membrane for oligopeptides, and paracellular passive diffusion for both (Caetano-Silva, Netto, Bertoldo-Pacheco, Alegría, & Cilla, 2020; Wada & Lönnerdal, 2014; Zhang, Ding, & Li, 2021). Therefore, it is possible that peptides keep their structural integrity, remaining bioactive for action in the human body. Spent yeast peptides have been mainly described by their antihypertensive, antioxidant and antimicrobial effects, becoming popular in the agri-food sector (Oliveira, Ferreira, Pereira, Pintado, & Carvalho, 2022b). Recently, Oliveira et al. (2022c) also demonstrated the cholesterol-lowering capacity of spent yeast peptides via the inhibition of 3-hydroxy-3-methylglutaryl coenzyme A (HMG-CoA) reductase. Nevertheless, some authors even defend the possibility of some Fe amount may be absorbed by the same peptide route, since it is not well-known in what manner Fe is absorbed when is bound with organic molecules (Caetano-Silva et al., 2020).

This study aimed to evaluate the performance of Fe-peptide complexes produced from spent yeast during *in vitro* GIT, by calculating the amount of bioaccessible Fe at the end of intestinal phase, together with protein amount and peptides molecular weight (MW) profile. Following in *vitro* GIT simulation, Caco-2 cells were exposed to the digested samples to evaluate the Fe uptake and ferritin (FER) production in enterocytes, so as to understand the potential of complexes to increase Fe bioavailability. Finally, several bioactive properties of remaining digested peptides were measured, namely antioxidant, antihypertensive and *anti*-cholesterolemic, in an attempt to combine a promising Fe-delivery ingredient with peptides' biological value in a single product. A Fe-bisglycinate benchmark and an inorganic Fe salt were added to the study, enabling a comparative performance of our complexes with alternatives of Fe supplementation. To the best of our knowledge, this is the first time that the INFOGEST protocol for *in vitro* human gastrointestinal tract simulation was exploited for the assessment of Fe-complex absorption and the evaluation of bioactive properties of remaining complex peptides after GIT.

2. Material and methods

2.1. Production of peptide fraction

Waste streams resulting from β-glucan extraction from engineered spent yeast (*Saccharomyces cerevisiae*) were used to produce a peptide rich-fraction through 1 kDa ultrafiltration and diafiltration, as detailed in Oliveira et al. (2022).

2.2. Synthesis of Fe-peptide complexes

Following the optimization of the Fe complexation conditions, described in Oliveira et al. (2023), Fe-peptide complexes were synthetised using a protein:Fe ratio of 2:1 (w/w) at pH 6.0, during 30 min, under anoxic conditions. Soluble Fe in the complexes was evaluated by Inductively Coupled Plasma Optical Emission spectroscopy (ICP-OES) immediately before their freeze-drying.

2.3. In vitro simulation of human gastrointestinal digestion

In order to assess the gastrointestinal performance of Fe-peptide complexes in comparison with different alternatives for Fe supplementation, "Gentle Fe" (Fe bisglycinate 20 mg) benchmark (Solgar, Leonia, NJ, USA) and an inorganic Fe salt in the form of ferrous sulphate ($FeSO_4{\cdot}7H_2O$; Sigma-Aldrich, Inc., St. Louis, USA) were used in this study. The three different Fe formulations were submitted to an *in vitro* simulation of human gastrointestinal digestion, as adapted from Brodkorb et al. (2019) (INFOGEST protocol). The amount of Fe was homogenized among all formulations according to recommended daily doses of "Gentle Fe" for adults: 1 capsule *per* day, which is equivalent to 20 mg of Fe. Therefore, Fe-peptide complexes and Fe salt were weighted and placed into acid-resistant hydroxypropyl methylcellulose (HPMC) capsules (Qualicaps, Whitsett, NC, USA) up to a total Fe concentration of 200 mg/L in INFOGEST protocol. Likewise, according to the information provided by the manufacturer, the benchmark was also encapsulated in HPMC capsules, using the mixture of bulking and anti-caking agents present in the formulation of Fe-bisglycinate. A GIT digestion with empty capsules (without any Fe content) was also performed to be used as negative control. Since Fe-peptide complexes are administered in capsule format, the oral phase was skipped, and the digestion was started at the gastric level. Samples were diluted in Simulated Gastric Fluid (SGF) (KCl, 6.9 mM; KH_2PO_4, 0.9 mM; $NaHCO_3$, 25 mM; NaCl,

47.5 mM; $MgCl_2$, 0.12 mM; $(NH_4)_2CO_3$, 0.5 mM; HCl, 15.6 mM) (Sigma-Aldrich, Inc., St. Louis, USA) and water in a ratio of 1:1 (v/v), adjusted to pH 3.0 with HCl 6 M, and $CaCl_2(H_2O)_2$ (Sigma-Aldrich, Inc., St. Louis, USA) was added to a final concentration of 0.15 mM. Then, a freshly prepared pepsin solution (Pepsin from porcine gastric mucosa powder ≥250 U/mg solid, Sigma-Aldrich, Inc., St. Louis, USA) was added in order to achieve an activity of 2000 U/mL and the samples were incubated and stirred for 2 h at 37 °C. At the end of gastric digestion, Simulated Intestinal Fluid (SIF) (KCl, 6.8 mM; KH_2PO_4, 0.8 mM; $NaHCO_3$ mM, 85; NaCl, 38.4 mM; $MgCl_2$, 0.33 mM; HCl, 8.4 mM) (Sigma-Aldrich, Inc., St. Louis, USA) solution was added to the volume of previous gastric digested samples in order to obtain a 1:1 ratio (v/v) and pH was adjusted to 7.0 using NaOH 6 M. Bile salt solution (Bile extract porcine, Sigma-Aldrich, Inc., St. Louis, USA) was added to archive a 10 mM concentration and $CaCl_2(H_2O)_2$ to a final concentration of 0.6 mM. Then, the pancreatin solution (Pancreatin from porcine pancreas, Sigma-Aldrich, Inc., St. Louis, USA) was added to a final concentration of 2000 U/mL and samples incubated and stirred for 2 h at 37 °C. At the end of intestinal phase, samples were heated for 10 min at 80 °C for enzymatic inactivation and then stored at −20 °C until further analysis.

Regarding the study of the bioactivities of the peptides comprised in the complexes and the benchmark, new samples without Fe content were also digested using the GIT protocol: a) "Gpep>1": peptide extract used for complex production in the same amount presented in Fe-peptide complexes capsules, and b) "Gly": glycine, in the same amount presented in "Gentle Fe" capsules. A GIT digestion without sample was also performed to be used as negative control ("GIT blank").

2.4. Fe uptake using a Caco-2 monolayer

2.4.1. Cell culture

Human colon carcinoma (Caco-2) cells were provided from American Type Culture Collection (HTB-37, VA, USA) and grown at 37 °C in a humidified atmosphere of 95% air and 5% CO_2 using high glucose (4.5 g/L) Dulbecco's Modified Eagle's Medium (DMEM) supplemented with 10% (v/v) heat-inactivated fetal bovine serum (Thermo Fisher Scientific, MA, USA), 1% (v/v) penicillin–streptomycin–fungizone (Lonza, Verviers, Belgium), and 1% (v/v) of non-essential amino acids 100 × (Sigma-Aldrich, St. Louis, USA). Cells were used between passages 26 and 29.

2.4.2. Cell viability

Cells were seeded at 1×10^4 cells/well in a 96-well microplate and, after overnight incubation at 37 °C, cells were exposed to GIT samples. Samples were filtrated (ø = 0.45 μm) to eliminate insoluble material resulting from GIT, so that Caco-2 cells were only exposed to soluble sample fractions. Cells were exposed to decreasing concentrations and different Fe concentrations were observed between the initial samples (Table 1, **dilution 0**) since they correspond to bioaccessible Fe fractions at the end of GIT (Table 2). Bioaccessible Fe concentrations and the corresponding successive dilutions in fresh medium are presented in Table 1.

Prestoblue® (Invitrogen, Massachusetts, USA) assay was conducted

Table 1
Bioaccessible Fe concentration (mg/L) of GIT samples and successive dilutions performed for Prestoblue® assay.

Dilution	*GIT control*	*Fe-peptide complex*	*Fe salt*	*Benchmark*
5	NA	0.154	0.218	3.08
4	NA	0.308	0.436	6.17
3	NA	0.616	0.873	12.3
2	NA	1.23	1.75	24.7
1	NA	2.47	3.49	49.4
0	NA	4.74	6.98	98.7

NA – Not applicable.

Table 2
Final soluble Fe concentration (mg/L) in samples after *in vitro* GIT simulation and its percentage (%) in comparison with initial protocol concentration (200 mg/L).

	GIT control	Fe-peptide complex	Fe salt	Benchmark
Soluble (mg/L)	0.741 ± 0.138	4.74 ± 0.31	6.98 ± 0.30	98.7 ± 1.1
% of initial content	NA	2.37 ± 0.15	3.49 ± 0.15	49.3 ± 0.6*

Results are expressed at average ± standard deviation ($n = 2$). *Statistically significantly higher than Fe-peptide complex and Fe salt ($p < 0.05$). NA-non appliable.

in order to evaluate cells' viability before performing Fe uptake assay, accordingly to the ISO 10993–5:2009 standard (International Organization for Standardization, 2009). Dimethyl sulfoxide (DMSO; Sigma-Aldrich, St. Louis, USA) at 10% (v/v) in culture media was used as death control and plain culture media was used as growth control. After 24 h-exposure, the PrestoBlue® reagent was added to each well and incubated for 2 h. Fluorescence was recorded (excitation 570 nm; emission 610 nm) after incubation using a microplate reader (Synergy H1, Biotek Instruments, Winooski, USA). All assays were performed in quadruplicate.

2.4.3. Fe uptake

Caco-2 cells were seeded at 1.5×10^5 cells/mL in cell culture inserts with 0.4 μm transparent PET membranes (Corning, NY, USA) placed within 6-well microplates. At each well, 2 mL of cell suspension were added to the apical chamber, whereas 2.5 mL of medium were inserted into the basal chamber. The content of apical and basal chambers was replaced with fresh medium every 2 d until usage (2 mL and 2.5 mL, respectively). Cell culture was kept for 14 more days for differentiation (Lea, 2015).

After 14 days, cells were washed with warm phosphate-buffered saline (PBS) buffer and exposed to GIT samples in apical chamber, with a soluble Fe concentration adjusted to 50 μM (Sharma, Shilpa Shree, Arora, & Kapila, 2017; Shilpashree, Arora, Kapila, & Sharma, 2020), as this concentration did not show alterations in Caco-2 viability. Before the dilution in fresh medium, the initial GIT samples were filtered (using sterile syringe filters, ø = 0.22 μm (Sartorius, Gottingen, Germany)) to obtain only the soluble Fe fraction, since this is the bioaccessible amount to be potentially absorbed by enterocytes. A volume of 2.5 mL of fresh medium was added to the basal chamber and after 2 h of exposure, the solutions from apical and basal chambers were collected for determination of Fe transport across the Caco-2 monolayers by ICP-OES. Fresh medium was added to both chambers, after washing the cells with warm PBS, that were then returned to the incubator for an additional 22 h period to allow FER synthesis (section 2.4.4). Afterwards, the content of both compartments was collected for Fe analysis, since the amount of Fe uptake by enterocytes during the exposure time (2 h) might be expelled for the medium until the end of period incubation (24 h). Additionally, to a GIT negative control (GIT sample without Fe content), a plain media control (unexposed cells) was also used in the assay. The Fe uptake by enterocytes was calculated using Equation 1a:

$$Fe\ uptake\ ratio = \frac{\frac{[Fe]_i - [Fe]_{2h}}{[Protein]}}{[Fe]_i} \quad (1)$$

where $[Fe]_i$ is the Fe concentration in the initial samples, $[Fe]_{2h}$ is the Fe concentration of collected samples after 2 h exposure, and [Protein] is the cell well protein concentration. Results are expressed as ng Fe/ng initial Fe. Mg protein. The assay was performed in sextuplicate.

2.4.4. Ferritin production

After incubation, cells were washed with cold PBS and scraped with 3 mL of cold 0.5 M EDTA-PBS solution (pH 8.0), the solution was collected, and the process repeated with 1 mL. Samples were then centrifuged (685×*g*, 20 min, 4 °C) and the supernatants were discarded. The cell pellets were resuspended in 300 μL of ice-cold lysis buffer (0.5 M EDTA-PBS with 1% v/v Triton X-100 (Sigma-Aldrich, St. Louis, USA)) and incubated on ice for 1 h. Cell lysates were centrifuged again (18,516×*g*, 30 min, 4 °C) and the supernatants were collected. Cell protein content was evaluated by the Bradford method (Bradford, 1976) using BSA (bovine serum albumin) (Thermo Fisher Scientific Inc., Massachusetts, USA) for calibration.

The FER synthesis by Caco-2 was evaluated in the cell lysates using the Human Ferritin ELISA Kit (RAB0197; Sigma-Aldrich, St. Louis, USA) according to manufacturer's instructions. The amount of FER synthesized by the cells was determined using Equation (2):

$$FER\ synthesis = \frac{[FER_p]}{[Protein]} \quad (2)$$

where [FER_p] is the FER produced amount, after 24 h since the initial exposure, and [Protein] is the cell protein content, and results were expressed in ng FER/mg protein. The assay was performed in sextuplicate.

2.5. Chemical characterization of GIT samples

2.5.1. Protein content

Protein quantification of samples, before and after GIT protocol, and GIT negative control, was carried out by the Dumas method (Dumas, 1831) using a Dumatec™ 8000 equipment (Foss, Hilleroed, Denmark). The analysis was performed at flow rates of 195 mL/min and 300 mL/min of helium and oxygen, respectively, at 1100 mbar. The protein content was calculated using a calibration curve from 10 mg to 150 mg of EDTA calibration standard (Foss, Hilleroed, Denmark) and estimated from the total nitrogen (N_2) using a multiplication factor of 6.25 (AOAC, 2005).

2.5.2. Protein and peptides MW

The protein and peptide MW distribution of Fe-peptide complexes, before and after GIT protocol, and negative GIT control, was performed according to the procedure described by Oliveira et al. (2022), using a system of ultra-high-performance liquid chromatography from Bruker Elute series, coupled to an ultrahigh-resolution quadrupole−quadrupole time-of-flight (UHR−QqTOF) mass spectrometer (Impact II; Bruke Daltonik GmbH, Bremen, Germany). An intensity Solo 2 C^{18} column (100 × 2.1 mm, 2.2 μm, Bruker Daltonik GmbH, Bremen, Germany) (BRHSC18022100) was used for separation and the detection by mass spectrometry was applied at positive mode from 150 to 2200 m/z. Post-acquisition internal mass calibration was employed at each analysis applying ESI-Low Concentration Tuning Mix (Agilent Technologies Inc., Santa Clara, CA, USA).

Before UHR−QqTOF analysis, peptides were concentrated and the Fe was eliminated, using SPE Lichrolut EN cartridges (40–120 μm, 500 mg, 6 mL) (Merck KGaA, Darmstadt, Germany). These were first preconditioned with acetonitrile and water before loading 15 mL of sample (2.5 g protein/mL). Peptides were eluted with 5 mL of acetonitrile and then injected.

2.5.3. Fe determination

Determination of Fe in Fe-peptide complex, benchmark and Fe salt, before and after GIT and Caco-2 cell exposure, was based on the methodology described by Chatelain, Pintado, Vasconcelos, E.Pintado, and Vasconcelos (2014) with some modifications. An optical emission spectrometer Model Optima 7000 DV ™ ICP-OES (Dual View, PerkinElmer Life and Analytical Sciences, Shelton, CT, USA) with radial configuration was used, being the concentration calculated by Fe standard calibration curve from 0.05 to 10 mg/L of commercial mix standard for ICP analysis (Inorganic Ventures, Christiansburg, USA). The measures were done in triplicate. Microwave digestion of samples was conducted in a speedwave XPERT (Berghof Products + Instruments GmbH, Eningen, Germany) before ICP analysis.

2.6. Biological activity of GIT samples

2.6.1. Angiotensin converting enzyme (ACE) inhibition assay

The ACE inhibition assay was performed according to Amorim et al. (2019) using o-Abs-Gly-p-nitro-Phe-OH trifluoroacetate salt (Bachem, Bubendorf, Switzerland) as substrate and 42 mU/mL of ACE (peptidyl-dipeptidase A from rabbit lung) (Sigma- Aldrich, St Louis, USA). The ACE inhibition (%) was calculated using Equation (3):

$$ACE\ inhibition = \frac{F_{control} - F_{sample}}{F_{control}} \times 100 \quad (3)$$

where $F_{control}$ and F_{sample} are the fluorescence of control (maximum ACE activity) and sample, respectively. The assay was performed in triplicate.

2.6.2. Antioxidant capacity

2.6.2.1. Scavenging activity using 2,2′-azinobis (3-ethyl-benzothiazoline-6-sulphonate)-radical cation ($ABTS^{\bullet+}$). The $ABTS^{\bullet+}$ scavenging activity was assessed by the method described by Gonçalves et al. (2019) with some modifications for a 96-well plate scale (Oliveira et al., 2022e) The percentage of $ABTS^{\bullet+}$ scavenging activity was calculated using Equation (4):

$$ABTS^{\bullet+}\ scavenging\ activity = \frac{A_{control} - A_{sample}}{A_{control}} \times 100 \quad (4)$$

where $A_{control}$ and A_{sample} are the absorbances of control and sample, respectively. The Trolox standard curve (50–560 μM) (Sigma-Aldrich, Inc., St. Louis, USA) was used to express Trolox Equivalent (TE) antioxidant activity of samples (μmol/g protein). The assay was performed in triplicate.

2.6.2.2. Scavenging activity using 2,2-diphenyl-1-picrylhydrazyl-free-radical ($DPPH^{\bullet}$). $DPPH^{\bullet}$ scavenging activity was carried out according to Prior, Wu, and Schaich (2005) with some modifications for a 96-well microplate scale (Oliveira et al., 2022). The percentage of $DPPH^{\bullet}$ scavenging activity was calculated using Equation (5):

$$DPPH^{\bullet}\ scavenging\ activity = \frac{A_{control} - A_{sample}}{A_{control}} \times 100 \quad (5)$$

where $A_{control}$ and A_{sample} are the absorbances of control and sample, respectively. The Trolox standard curve (7.5–240 μM) was used to express TE antioxidant activity of samples (μmol/g protein). The assay was performed in triplicate.

2.6.2.3. Oxygen radical absorbance capacity (ORAC). ORAC assay was assessed as described by Coscueta, Campos, Osório, Nerli, and Pintado (2019). The area under curve (AUC) was calculated for each sample by integrating the relative fluorescence curve and the Trolox standard curve (10–80 μM) was used to express TE antioxidant activity of samples (μmol/g protein). The assay was performed in triplicate.

2.6.3. HMG-CoA (3-hydroxy-3-methylglutaryl coenzyme A) reductase inhibition assay

HMG-CoA Reductase Activity Assay Kit (colorimetric) (Abcam, Cambridge, United Kingdom) was used for assessing the HMG-CoA reductase inhibition according to the manufacturer's guidelines. The

method measured the decrease of absorbance at 340 nm in a microplate reader, during 15 min, which resulted from the consumption of NADPH by the enzyme. Two time points within the linear range, and with a minimum of 2 min apart, of absorbance were used for calculations of the HMG-CoA reductase activity (units/mg protein) and the HMG-CoA reductase inhibition (%), as recommended by the manufacturer. Atorvastatin was used as a reference drug inhibitor and Pravastatin as a commercial inhibitor (control). The assay was performed in triplicate in two independent plates.

2.7. Statistical analysis

The statistical analysis was performed using the Real Statistics Resource Pack software (Release 7.2). Outliers were excluded using the interquartile range with multiplier of 2.2 and data normality was checked using the Shapiro-Wilk test. Fe and FER results from different groups of Caco-2 uptake assay were subjected to the analysis of variance (ANOVA) followed by Tukey's post hoc test.

3. Results and discussion

3.1. In vitro simulation GIT of Fe-peptide complex, Fe salt and benchmark

3.1.1. Fe bioaccessible (%)

The soluble Fe content of samples subjected to simulated *in vitro* GIT were analysed at the end of the intestinal phase, since this fraction corresponds to its bioaccessible fraction which can potentially be absorbed by the duodenal enterocytes (Table 2).

This fraction was obtained by filtrating the suspended solid particles from the digested samples (ø = 0.45 μm) obtained during GIT protocol. Since initial GIT samples were prepared to obtain a Fe concentration of 200 mg/L, it was observed that benchmark showed the highest percentage of bioaccessible Fe (49.3 ± 0.6% from the initial), followed by Fe-peptide complex (2.37 ± 0.15%) and Fe salt (3.49 ± 0.15%), with no significant differences between them. Despite the expectations, a negligible concentration of soluble Fe was observed in GIT control (Table 1), which can be related with impurities of enzymatic solution reagents used in GIT protocol, since pepsin, pancreatin and bile are powder extracts derived from porcine (Sigma-Aldrich, Inc., St. Louis, USA).

Since all samples were submitted to GIT simulation in acid resistant HPMC capsules, the behaviour of Fe salt followed the expected pattern, where on intestine environment, the Fe salt was released from the capsule and the soluble Fe may precipitate, making it unavailable to be absorbed. This result was in accordance to Wang et al. (2011), which obtained a percentage of Fe-release above 5% at pH 7.0 for $FeSO_4$. Otherwise, the small amount of bioaccessible Fe in the peptide complex sample was not expected, since the binding should have protected the mineral from becoming insoluble under intestinal conditions, as occurred with the benchmark, where almost 50% of Fe was bioaccessible (Table 2). The reported benchmark results for ferrous bisglycinate are consistent with those from previous studies, which showed an absorption rate of approximately 40% (Lin et al., 2021). These data suggests that HPMC capsules used for preparation of Fe salt and complexes for GIT protocol seem not to be the most suitable material. In fact, it has been shown that HPMC is capable of absorbing Fe^{3+} in a pH range of 3.0–7.0 from 100 to 1000 ppm (Sözügeçer & Bayramgil, 2013). For this reason, it is therefore possible that Fe^{2+} may also be absorbed into the HPMC solid debris. This potential HPMC adsorption of Fe was not observed for benchmark, possibly due to differences in the capsules characteristics, although both are reported having the same base material. The use of bulking agents on the benchmark formulation may also have protected Fe from becoming insoluble during the GIT protocol, being responsible for its high bioaccessible fraction in relation to complexes.

On the other hand, another possible explanation for the low amount of bioaccessible Fe in our complex may be related with peptide degradation during intestinal GIT phase, when the capsule content is released. In fact, complexation reaction increases Fe solubility and bioavailability, if the peptides chosen for the reaction are digestion-resistant to protect Fe through the chemical changes along GIT (Caetano-Silva et al., 2020). Although the stomach's low pH will increase Fe solubility, since its reduced form (Fe^{2+}) is promoted, the protonation of Fe-binding sites will weaken the metal-peptide bounds, which may lead to Fe release from peptides before they arrive at the duodenum to be absorbed (Caetano-Silva et al., 2020). For this reason, and limiting the potential mineral interaction with food components, acid-resistant capsules were used in the present study as reported by other authors (Bryszewska, 2019; Filiponi, Gaigher, Caetano-Silva, Alvim, & Pacheco, 2019).

At intestinal pH, the Fe-peptide bounds are favoured because of the deprotonation of peptides amino acids residues' carboxyl groups, increasing complex stability. However, if peptides used were less efficient in binding Fe at this phase, some non-complexed Fe could precipitate, since free Fe solubility decrease at duodenum alkaline pH, making it unavailable to be absorbed. Indeed, similar preliminary results were previously observed, when increasing the pH of complex production from 6.0 to 7.0 lead to a decrease in soluble Fe from 88.0% to 53.4% (Oliveira et al., 2023). For this reason, the Fe released from peptides at this stage may be bound to other molecules of GIT solutions (Caetano-Silva, Cilla, Bertoldo-Pacheco, Netto, & Alegría, 2018), turning insoluble and thus not bioaccessible. Indeed, the strength of Fe-peptide bound is the key: it must be strong enough to prevent Fe release before duodenum, preventing its complexation with other diet components, but, at the same time, weak enough to allow the Fe release to be transported by carriers in the apical site of enterocytes (Caetano-Silva et al., 2020).

3.1.2. Protein profile

In an attempt to evaluate the protein profile of Fe-peptides complexes, before and after digestion, analysis of peptides MW and protein content (%) were performed.

Before GIT, the percentage of peptides <1500 Da rounded about 85% (Fig. 1), which is of particular relevance, as peptides with MW between 300 and 1500 Da are described to hold higher affinity for binding with Fe (Wu et al., 2020). After GIT, this percentage increased to 98%, as expected, due to the degradation of the peptides under GIT's different conditions. The decrease of complexed peptides size during simulated GIT was already reported by Lin et al. (2021). For this reason, it would be important to explore how this degradation may affect the binding Fe-peptides, as well as study other peptide features as structure, amino acid composition and steric effects, in order to understand how the binding strength of Fe-peptides in complexes production can be improved to make Fe from complexes at the end of intestinal phase more bioaccessible to be absorbed (Gómez-Grimaldos et al., 2020). However, these analyses were not performed in this work since Fe-peptide complexes were prepared using a peptide-rich extract originating from a yeast by-product that, despite containing 67.2% of protein (w/w), was also composed of other components, such as sugars and residual minerals (Oliveira et al., 2022). These components hinder the possible evaluation of the peptide sequence and, consequently, the study of the complexes' binding mechanism. In fact, in a similar study, Athira et al. (2021) were not successful in reaching a conclusion about the binding mechanism and how this may influence the Fe bioaccessibility at different chemical environment during GIT, as they identified too many amino acid sequences in the used whey protein hydrolysates. On the other hand, some authors included chromatographic processes for peptides or complexes purification, thus making the identification of amino acid sequences and their potential sites for mineral binding easier (Caetano-Silva et al., 2015; Wu et al., 2017). However, the inclusion of this additional step would drastically increase the complex production cost, making it not cost-effective (Oliveira et al., 2022a), Oliveira et al., 2022bnd, for that reason, it was not considered in the present study.

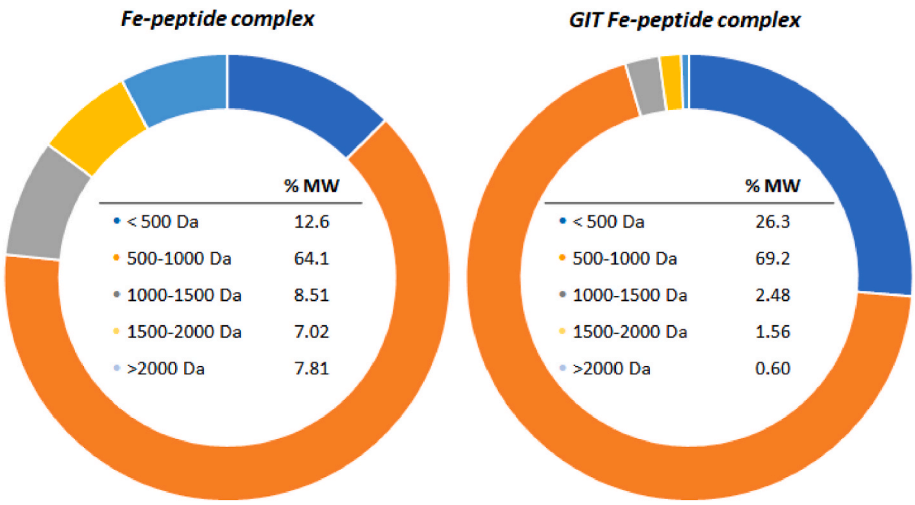

Fig. 1. Peptides molecular weight distribution (% MW) in Fe-peptide complex before (left) and after (right) *in vitro* GIT simulation.

Regarding the protein content, the initial amount on Fe-peptide complex (20.8 ± 0.9%; w/w) was enhanced to 45.5 ± 2.0% after digestion. However, it must be pointed out that the main contributor for this increase was the enzymatic cocktail used in GIT protocol, since the final protein content of other samples subjected to the same digestion procedure have similar results (GIT control: 45.3 ± 0.2%, Fe salt: 44.2 ± 0.9% and benchmark: 43.6 ± 1.3%). Indeed, the same tendency was observed in benchmark, since the protein percentage increased from 17.7 ± 0.7% to 43.6 ± 1.3% with GIT.

3.2. Fe uptake study

After the determination of bioaccessible Fe following the GIT simulation, the evaluation of the amount that enters in duodenal enterocytes (bioavailable Fe) is fundamental, because the condition "higher bioaccessibility, higher bioavailability" is not always observed (Caetano-Silva et al., 2020). For this reason, an *in vitro* model using a Caco-2 monolayer was exploited to evaluate Fe uptake of the Fe-peptide complexes, "Gentle Fe" benchmark and Fe salt samples, together with negative GIT control (without any Fe content). Caco-2 cells have been described as the reference *in vitro* model, since this cell line spontaneously differentiates, acquiring similar characteristics to mature enterocytes, thus acting as the intestinal mucosa barrier and simulating the absorption conditions in humans. Moreover, this cell line has been shown to be suitable for food Fe bioavailability studies (Gómez-Grimaldos et al., 2020) since it occurs via the divalent metal-ion transporter-1 (DMT1) that is expressed in the apical side of these enterocytes.

3.2.1. Cell viability

Before the uptake assay, Caco-2 were exposed to filtered GIT samples for 24 h, according to ISO 10993–5:2009 protocol (International Organization for Standardization, 2009), to understand the effect of GIT matrix on cells and to select a non-cytotoxic concentration for the Fe uptake protocol. The toxicity of Fe^{2+} is related to the excessive production of free radicals, which influence cell membrane stability, leading to the initiation of lipid peroxidation and DNA damage. However, some authors have described a toxicity decrease when Fe^{2+} is bound to the peptides (Eckert et al., 2016).

Regarding the Fe concentrations of exposure (Table 1), Caco-2 metabolism was inhibited by more than 30% (30.1–68.4%) only when exposed to direct GIT samples (dilution 0), which means that these concentrations are cytotoxic and cannot be used in the subsequent assay. Despite the fact all diluted samples displayed no cytotoxic effects against Caco-2, Fe concentration was adjusted to 50 μM for the uptake assay, as suggested by other authors (Sharma et al., 2017; Shilpashree et al., 2020), which is equivalent to 2.8 mg/L of Fe. The GIT control sample was also diluted for uptake assay, used as control of GIT matrix, based on dilution of Fe-peptide complexes. The non-cytotoxic profile of the diluted samples (Table 1, dilution 1 to 5) are in accordance to Wang et el. (2014) since they did not observe a significant decrease of Caco-2 viability from 10 to 50 mg/L Fe of digested lactoglobulin hydrolysate-Fe complexes.

3.2.2. Fe uptake and FER production

After 14 days of cells differentiation to allow for a monolayer formation and cell polarization, Fe uptake by Caco-2 was performed and the Fe was measured on initial exposure solutions (GIT samples diluted for 50 μM in fresh medium), and on solutions from apical and basal chambers after Caco-2 exposure (2 h and 24 h) by ICP-OES. However, after Fe analysis of initial samples, it was observed that Fe concentrations were not corresponding to the theoretical concentration of 50 μM prepared (2.8 mg/L) (Table 3).

These variations may be related to the formation of some precipitates during samples' freezing, since they were preserved at −20 °C after GIT until being used for Fe uptake protocol. The calculation of Fe uptake rate by enterocytes was performed by the difference of Fe concentration at initial samples, and apical after 2 h exposure, being normalized by initial exposure Fe for final calculation, to compare the results between the different samples. Indeed, the inclusion of this normalization step is essential for an accurate calculation since the exposure of enterocytes to higher Fe concentrations in some samples may influence the expression of genes involved in cellular Fe metabolism, which may subsequently promote or decrease Fe uptake (Kalgaonkar & Lönnerdal, 2009). The ratio of Fe:protein (ng Fe/ng initial Fe. Mg protein) was also used as an index of Fe uptake as a measure of normalization for the number of cells exposed.

The results of Fe uptake of Fe-peptide complexes, Fe salt and benchmark are presented in Fig. 2. On average, our Fe peptide complexes recorded higher ratios of Fe uptake than those recorded for Fe salt

Table 3
Fe concentration (mg/L) on initial samples of Caco-2 exposure (GIT samples theoretically diluted for 50 μM in fresh medium).

	Fe-peptide complexes	Control GIT	Fe salt	Benchmark
Initial Caco-2 exposure	0.750	< LOD	0.863	2.51

<LOD – below limit of detection.

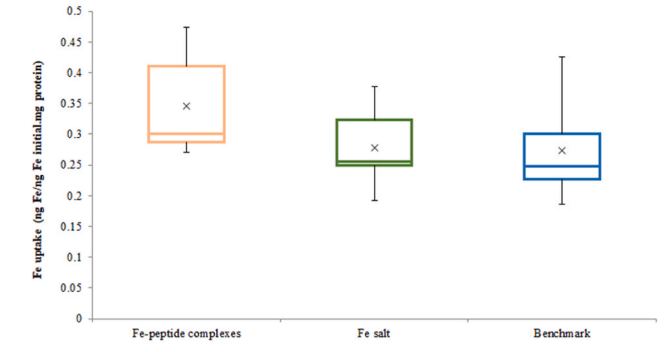

	Fe-peptide complexes	Fe salt	Benchmark
Average ± SD	0.346 ± 0.090	0.279 ± 0.069	0.274 ± 0.086

SD – Standard deviation

Fig. 2. Fe uptake by Caco-2 cells exposed to Fe-peptide complexes, Fe salt and benchmark. All samples were compared by Tukey's test ($n = 6$) and no statistically significant alterations were found ($p > 0.05$).

and benchmark. However, no statistically significant differences were found in Caco-2 Fe uptake between all samples ($p > 0.05$).

As expected, no Fe was detected in cell culture medium collected from Caco-2 control (<LOD). Fe was also not detected at basal samples (<LOD), meaning that it was stored inside the enterocytes, not being excreted for the extracellular medium. The same result was observed in fresh medium collected after 24 h exposure at apical and basal solutions, confirming this assumption.

Additionally, the FER produced in enterocytes was also quantified, since Caco-2 can synthesize this protein in response to high intracellular Fe levels (Shilpashree et al., 2020). Indeed, it was observed an increase of FER levels in cells exposed to the different Fe-containing samples (3.26–3.33 ng/mg protein) regarding cells exposed to GIT control (2.88 ± 0.08 ng/mg protein), evidencing that Fe enters the enterocytes and suggesting its transport by cell membrane and subsequent retention (Sharma et al., 2017), thus confirming our results for Fe uptake by Caco-2 (Fig. 2). These results are presented as FER produced in relation to GIT control cells in Fig. 3. However, no statistically significant alterations were found between Fe-peptide complexes, Fe salt and benchmark ($p > 0.05$) as shown by Fe uptake (Fig. 2). Since FER is a measure of Fe Caco-2 bioavailability, a correlation of FER levels and Fe uptake was explored using Pearson's method. However, no significant relation was found ($p > 0.05$).

Looking at the obtained results, it is possible to affirm that our Fe-peptide complexes led to an increase of Fe uptake and FER production. However, this increase appears trivial when compared to other

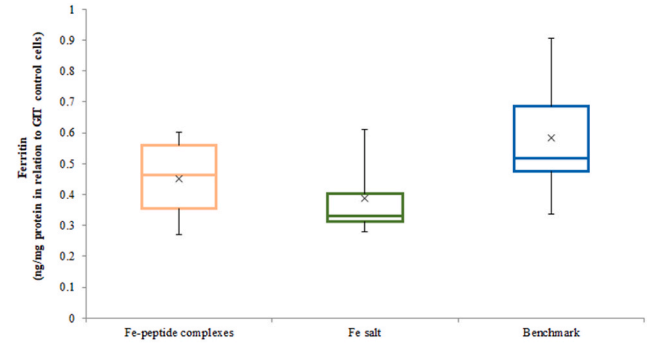

	Fe-peptide complexes	Fe salt	Benchmark
Average ± SD	0.450 ± 0.152	0.388 ± 0.150	0.584 ± 0.218

SD – Standard deviation

Fig. 3. Ferritin (FER) produced by Caco-2 cells exposed to Fe-peptide complexes, Fe salt and benchmark in relation to cells exposed to GIT control. All samples were compared by Tukey's test ($n = 6$) and no statistically significant alterations were found ($p > 0.05$).

studies that reported a significant Fe uptake and increase of FER synthesis by Caco-2 cells when exposed to digested Fe-peptide complexes, using natural peptides from different sources as ligands (Caetano-Silva et al., 2018; Chen et al., 2017; Eckert et al., 2016; Filiponi et al., 2019; García-Nebot, Barberá, & Alegría, 2013; Sharma et al., 2017; Shilpashree et al., 2020; Wang, Ai, Meng, Zhou, & Mao, 2014). A possible explanation for this difference may concern the different digestion protocols used. In fact, the abovementioned authors use comparatively simple digestions procedures, with demineralized digestive enzymes (pepsin and pancreatin-bile solutions) with the appropriate pH values readjusted. Differently, in this work, digestion of the samples was attained using the INFOGEST protocol (Brodkorb et al., 2019), recently developed by this international research network to better mimic the human physiological conditions and the complex digestion process that undergoes in the human digestive tract. This international standardized methodology requires, however, an elaborated GIT matrix comprising, among other elements, several electrolytes that may be affecting the different cellular mechanisms, such as their metabolism (e.g., ATP cell content and cell barrier integrity), by hyperosmotic stress (Grauso, Lan, Andriamihaja, Bouillaud, & Blachier, 2019), thus compromising the cells stimulation for Fe uptake and consequently FER synthesis. Furthermore, bile salts used in the GIT matrix, which are likely to still be present in samples, have been reported to hold emulsifying properties (Garner, Mills, Elias, & Neuberger, 1991; Neves et al., 2019), that can provoke cell membrane lysis. Nevertheless, as far as our knowledge extents, this has been the first time that the INFOGEST protocol was used for the digestion of Fe-peptide complexes. Furthermore, to the best of our knowledge, this has also been the first time that peptides from engineered spent yeast waste streams were used to evaluate Fe *in vitro* absorption from complexes, thus using a circular economy approach. Finally, different *in vitro* methodologies already described in literature, from GIT (Brodkorb et al., 2019) to Caco-2 exposure to Fe complexes (Caetano-Silva et al., 2018; Remondetto, Beyssac, & Subirade, 2004; Sharma et al., 2017; Shilpashree et al., 2020) have been combined and adapted in this work to develop alternative methodologies to understand the performance of our ingredient regarding other Fe supplementation alternatives.

The mechanism of Fe-peptide complexes' entry in the enterocyte is still unclear since it is not consensual how Fe is absorbed when bound to organic molecules. Some authors pointed out the DMT1 carrier as the main responsible, since it is expressed at apical site of enterocytes in human body, but other studies described the expression of other transporters which appear to function independently of DMT1 (Aly, López-Nicolás, Darwish, Frontela-Saseta, & Ros-Berruezo, 2016). On the other hand, the peptides' carrier PepT1, also expressed in the intestinal epithelium, may also be involved in Fe absorption since low MW peptides are bound to this mineral (Caetano-Silva et al., 2020).

FER synthesis has also been used to evaluate Fe uptake by enterocytes as an indirect measure since they synthesize this protein in response to increase intracellular Fe. This intracellular protein has the ability to store Fe, releasing this mineral in a controlled envFement when needed (Brissot & Loréal, 2016). However, the regulation of Fe absorption *in vivo* involves the communication of epithelium with other organs, such as liver via hepcidin production, which points out a limitation of using only Caco-2 cell line as *in vitro* model of Fe absorption (Scheers, Almgren, & Sandberg, 2014). For this reason, in spite of the Fe uptake and FER synthesis enhancement observed by our Fe-peptide complexes at Caco-2, it might be interesting to reproduce this study using co-culture models including hepatocytes (e.g. HepG2) for a closer physiological approach. Another co-cultured model that would better translate the complexity of the intestinal interface would consider a membrane seeded using a mucus-producing intestinal cell line (HT-29-MTX), since Laparra, Glahn, and Miller (2009) observed that mucin production can tightly regulate Fe absorption by modulating the expression of DMT1.

Given their performance, our Fe-peptide complexes, seem to be a

promising alternative for Fe dietary supplementation, since they had a similar behaviour to Fe salt and to the benchmark regarding the Fe uptake levels and FER synthesis (Figs. 2 and 3). In fact, complexes can be considered a better choice than Fe salt for supplementation, since the latter have the disadvantage of Fe-binding with absorption inhibitors during GIT, such as phytates and phenolics, that are usually present in a normal diet (Chen et al., 2017).

It was also demonstrated that high Fe bioaccessibility was not directly related to its high bioavailability, as the benchmark showed the highest value of soluble Fe after GIT (Table 2) but similar values of Fe uptake and FER production were observed when comparing to Fe-peptide complexes and Fe salt (Figs. 2 and 3). This hypothesis was already pointed out by other authors (Caetano-Silva et al., 2020) and is further corroborated in the present study.

3.3. Biological activity of GIT samples

$ABTS^{\bullet+}$ and FRAP activities of whey protein Fe-complexes have been reported to decrease after Fe complexation, regarding the original whey peptides, by Athira et al. (2021) thus, suggesting the influence of Fe on redox mechanisms of the methods used for bioactivity evaluation. For this reason, and assuming that Fe released from peptides at the end of GIT follows its pathway thus being absorbed into the blood, the remaining peptides of Fe-peptide complexes might remain bioaccessible in the human body and be absorbed as well. Regarding the "Gentle Fe" benchmark (Fe bisglycinate) the same assumption was taken, which would result in a substantial amount of free glycine bioaccessible at the end of GIT to be transported into the bloodstream. Following this assumption for both samples, and considering the importance of bioactive peptides in several physiological functions in the human body (Oliveira et al., 2022), new samples without Fe content were digested using the GIT protocol and their potential bioactivities for nutraceutical market were assessed. The results for antioxidant capacity, antihypertensive activity (ACE) and *anti*-cholesterolemic activity (HMG-CoA reductase inhibition) are presented in Table 4.

Regarding the antioxidant properties, all samples showed ability to reduce $ABTS^{\bullet+}$ but no significant differences were observed between GIT blank and samples (Supplementary material 1), which may suggest that Gpep> 1 and Gly do not present scavenging $ABTS^{\bullet+}$ activity. Likewise, it was not demonstrated scavenging $DPPH^{\bullet}$ activity of GIT blank or samples since the values found were below the method detection limit (Table 4). In fact, $ABTS^{\bullet+}$ is a more reactive radical than $DPPH^{\bullet}$ which may lead to unbiased results, being important supporting its results with other assays (Mareček et al., 2017). On the other hand, Gpep >1 presented the highest ORAC activity (761 ± 22 μmol TE/g protein), followed by Gly (357 ± 11 μmol TE/g protein) and blank (200 ± 8 μmol TE/g protein) ($p < 0.05$) (Supplementary material 1). The values obtained for Gpep>1 are in accordance to Xiao et al. (2022) and Conway, Gauthier, and Pouliot (2013), which studied antioxidant properties of chicken, buttermilk and whey protein hydrolysates. In fact, yeast peptides were already described by their antioxidant properties demonstrated by ORAC (Amorim et al., 2019; Costa et al., 2023). Nevertheless, glycine and its derivatives were also reported by their high scavenging activity (Kitts, 2021; Shen, Tebben, Chen, & Li, 2019; Suh, Lee, & Jung, 2003). which is according to their described human body protective effect against oxidative damage since this non-essential amino acid is used for glutathione synthesis (Díaz-Flores et al., 2013; Pérez-Torres, Zuniga-Munoz, & Guarner-Lans, 2016).

Indeed, the differences observed on the three scavenging activity assays may be related to their different mechanisms of oxidative chain reactions, producing different free radicals. Phenomena of redox mechanisms are involved in $ABTS^{\bullet+}$ and $DPPH^{\bullet}$ assays but the former involves the reduction of cation-radical $ABTS^{\bullet+}$ into ABTS by electron transference of an antioxidant, while $DPPH^{\bullet}$ is reduced by hydrogen atom donation of an antioxidant (Oliveira et al., 2022). On the other hand, ORAC assay is also based on hydrogen transference but its biologically more relevant than other scavenging assays because the radical generated, peroxyl, is also found in physiological conditions (Prior et al., 2003).

On the other hand, Gpep >1 did not show a higher inhibition of ACE and HMG-CoA reductase than the blank, which indicates that no antihypertensive and *anti*-cholesterolemic effects were found after GIT. In fact, in order to maintain their bioactive properties, peptides need to resist GIT degradation to reach the blood stream in an active form (Coscueta et al., 2019). However, in the present study, this may not be the main reason for the lack of these bioactive properties since only a small amount of peptides remains after GIT, being samples mainly composed by the protein content of GIT enzymatic matrix, which indicates that it may not be correct to relate the decrease of bioactivity to digested yeast peptides. Indeed, peptide rich-fractions from spent yeast (>1 kDa) already demonstrated HMG-CoA inhibition at 1.5 and 2.5 mg/mL (60–70%) and a IC50 of 1.5 mg/mL at ACE-inhibition assay (Oliveira et al., 2022), which suggests that the absence of effect may be influenced by the low peptides concentration.

Table 4
Antioxidant activity ($ABTS^{\bullet+}$, $DPPH^{\bullet}$ and ORAC), expressed as μmol Trolox Equivalent/g of protein, and inhibition percentage (%) of ACE and HMG-CoA reductase of GIT samples: blank, Gpep>1 and Gly.

	$ABTS^{\bullet+\dagger}$	ORAC	$DPPH^{\bullet}$	HMG-CoA†*	ACE†*
	μmol TE/g protein			% inhibition	
GIT blank	220 ± 42	200 ± 8	< LOQ	22.2 ± 7.9	40.3 ± 0.5
Gpep >1	238 ± 63	761 ± 22‡		33.3 ± 3.9	40.8 ± 1.9
Gly	231 ± 51	357 ± 11		36.1 ± 0.0	33.2 ± 1.1

Results are expressed in average ± standard deviation ($n = 3$). < LOQ – Below limit of quantification, TE - Trolox Equivalent. †No statistically significant alterations ($p > 0.05$). ‡ Statistically significant increase in comparison with GIT blank and Gly ($p < 0.05$). *For Caco-2 biocompatible extract concentration reported at Oliveira et al. (2022)

4. Conclusion

Fe-peptide complexes produced from spent yeast peptide-rich extracts showed potential to be a promising alternative for Fe dietary supplementation. After *in vitro* GIT simulation, the resulting bioaccessible Fe amount was absorbed by the duodenal enterocytes, resulting in the promotion of FER synthesis. Moreover, Fe complexes had a similar performance to Fe salt and a benchmark of Fe-bisglycinate, without having Fe salt's disadvantages of binding with food compounds during GIT and causing health problems, such as gastrointestinal irritations. Additionally, peptides from the complexes demonstrated antioxidant properties which may be important to protect Fe from oxidation during the different GIT environments. Further *in vivo* studies of Fe-peptide complexes should be conducted, since several compounds produced by other organs other than the intestine are involved in the Fe absorption mechanism.

CRediT authorship contribution statement

Ana Sofia Oliveira: Conceptualization, Investigation, Writing - Original Draft.
Carlos M.H. Ferreira: Investigation, Writing - Review & Editing.
Joana Odila Pereira: Investigation, Writing - Review & Editing.
Sara Silva: Investigation, Writing - Review & Editing.
Eduardo M. Costa: Investigation, Writing - Review & Editing.
Ana Margarida Pereira: Investigation, Writing - Review & Editing.
Margarida Faustino: Investigation.
Joana Durão: Investigation.
Manuela E. Pintado: Resources, Supervision, Project administration, Funding acquisition.
Ana P. Carvalho: Writing - Review & Editing, Supervision.

Declaration of competing interest

The authors declare that they have no known competing financial interests or personal relationships that could have appeared to influence the work reported in this paper.

Data availability

Data will be made available on request.

Acknowledgements

This work was co-financed by European Regional Development Fund (ERDF), through the Operational Program for Competitiveness and Internationalization (POCI) supported by Amyris Bio Products Portugal, Unipessoal Lda and Escola Superior de Biotecnologia—Universidade Católica Portuguesa through Alchemy project 'Capturing High Value from Industrial Fermentation Bio Products (POCI-01-0247-FEDER-027578)'.

Appendix A. Supplementary data

Supplementary data to this article can be found online at https://doi.org/10.1016/j.fbio.2023.103106.

References

Aly, E., López-Nicolás, R., Darwish, A. A., Frontela-Saseta, C., & Ros-Berruezo, G. (2016). Supplementation of infant formulas with recombinant human lactoferrin and/or galactooligosaccharides increases iron bioaccessibility as measured by ferritin formed in Caco-2 cell model. *Food Research International, 89*, 1048–1055. https://doi.org/10.1016/j.foodres.2016.08.030

Amorim, M., Marques, C., Pereira, J. O., Guardão, L., Martins, M. J., Osório, H., et al. (2019). Antihypertensive effect of spent brewer yeast peptide. *Process Biochemistry, 76*, 213–218. https://doi.org/10.1016/j.procbio.2018.10.004

Anderson, G. J., Lu, Y., Frazer, D. M., & Collins, J. F. (2018). Intestinal iron absorption. In *Reference module in biomedical Sciences* (2nd ed., pp. 1–11). Elsevier. https://doi.org/10.1016/B978-0-12-801238-3.65641-6.

Athira, S., Mann, B., Sharma, R., Pothuraju, R., & Bajaj, R. K. (2021). Preparation and characterization of iron-chelating peptides from whey protein: An alternative approach for chemical iron fortification. *Food Research International, 141*, Article 110133. https://doi.org/10.1016/j.foodres.2021.110133

Bradford, M. M. (1976). A rapid and sensitive method for the quantitation of microgram quantities of protein utilizing the principle of protein-dye binding. *Analytical Biochemistry, 72*(1–2), 248–254. https://doi.org/10.1016/0003-2697(76)90527-3

Brissot, P., & Loréal, O. (2016). Iron metabolism and related genetic diseases: A cleared land, keeping mysteries. *Journal of Hepatology, 64*(2), 505–515. https://doi.org/10.1016/j.jhep.2015.11.009

Brodkorb, A., Egger, L., Alminger, M., Alvito, P., Assunção, R., Ballance, S., et al. (2019). INFOGEST static *in vitro* simulation of gastrointestinal food digestion. *Nature Protocols, 14*(4), 991–1014. https://doi.org/10.1038/s41596-018-0119-1

Bryszewska, M. (2019). Comparison study of iron bioaccessibility from dietary supplements and microencapsulated preparations. *Nutrients, 11*(2), 273. https://doi.org/10.3390/nu11020273

Caetano-Silva, M. E., Bertoldo-Pacheco, M. T., Paes-Leme, A. F., & Netto, F. M. (2015). Iron-binding peptides from whey protein hydrolysates: Evaluation, isolation and sequencing by LC-MS/MS. *Food Research International, 71*, 132–139. https://doi.org/10.1016/j.foodres.2015.01.008

Caetano-Silva, M. E., Cilla, A., Bertoldo-Pacheco, M. T., Netto, F. M., & Alegría, A. (2018). Evaluation of *in vitro* iron bioavailability in free form and as whey peptide-iron complexes. *Journal of Food Composition and Analysis, 68*(October 2016), 95–100. https://doi.org/10.1016/j.jfca.2017.03.010

Caetano-Silva, M. E., Netto, F. M., Bertoldo-Pacheco, M. T., Alegría, A., & Cilla, A. (2020). Peptide-metal complexes: Obtention and role in increasing bioavailability and decreasing the pro-oxidant effect of minerals. *Critical Reviews in Food Science and Nutrition, 0*(0), 1–20. https://doi.org/10.1080/10408398.2020.1761770

Chatelain, P. G., Pintado, M. E., & Vasconcelos, M. W. (2014). Evaluation of chitooligosaccharide application on mineral accumulation and plant growth in *Phaseolus vulgaris*. *Plant Science, 215–216*, 134–140. https://doi.org/10.1016/j.plantsci.2013.11.009

Chen, Q., Guo, L., Du, F., Chen, T., Hou, H., & Li, B. (2017). The chelating peptide (GPAGPHGPPG) derived from Alaska pollock skin enhances calcium, zinc and iron transport in Caco-2 cells. *International Journal of Food Science and Technology, 52*(5), 1283–1290. https://doi.org/10.1111/ijfs.13396

Collins, J. F., & Anderson, G. J. (2012). Molecular mechanisms of intestinal iron transport. In *Physiology of the gastrointestinal tract (first edit, vol. 2, pp. 1921–1947)*. Elsevier. https://doi.org/10.1016/B978-0-12-382026-6.00071-3.

Conway, V., Gauthier, S. F., & Pouliot, Y. (2013). Antioxidant activities of buttermilk proteins, whey proteins, and their enzymatic hydrolysates. *Journal of Agricultural and Food Chemistry, 61*(2), 364–372. https://doi.org/10.1021/jf304309g

Coscueta, E. R., Campos, D. A., Osório, H., Nerli, B. B., & Pintado, M. (2019). Enzymatic soy protein hydrolysis: A tool for biofunctional food ingredient production. *Food Chemistry X, 1*, Article 100006. https://doi.org/10.1016/j.fochx.2019.100006

Costa, E. M., Oliveira, A. S., Silva, S., Ribeiro, A. B., Pereira, C. F., Ferreira, C., et al. (2023). Spent yeast waste streams as a sustainable source of bioactive peptides for skin applications. *International Journal of Molecular Sciences, 24*(3), 2253. https://doi.org/10.3390/ijms24032253

Díaz-Flores, M., Cruz, M., Duran-Reyes, G., Munguia-Miranda, C., Loza-Rodríguez, H., Pulido-Casas, E., et al. (2013). Oral supplementation with glycine reduces oxidative stress in patients with metabolic syndrome, improving their systolic blood pressure. *Canadian Journal of Physiology and Pharmacology, 91*(10), 855–860. https://doi.org/10.1139/cjpp-2012-0341

Dumas, J. B. A. (1831). *Procedes de l'analyse organique* (pp. 198–205). Annales de Chimie et de Physique.

Eckert, E., Lu, L., Unsworth, L. D., Chen, L., Xie, J., & Xu, R. (2016). Biophysical and in vitro absorption studies of iron chelating peptide from barley proteins. *Journal of Functional Foods, 25*, 291–301. https://doi.org/10.1016/j.jff.2016.06.011

Ferreira, C., Pereira, C. F., Oliveira, A. S., Faustino, M., Pereira, A. M., Durão, J., et al. (2022). A step for the valorization of spent yeast through production of iron–peptide complexes—a process optimization study. *Processes, 10*(8), 1464. https://doi.org/10.3390/pr10081464

Filiponi, M. P., Gaigher, B., Caetano-Silva, M. E., Alvim, I. D., & Pacheco, M. T. B. (2019). Microencapsulation performance of Fe-peptide complexes and stability monitoring. *Food Research International, 125*(November 2018), Article 108505. https://doi.org/10.1016/j.foodres.2019.108505

García-Nebot, M. J., Barberá, R., & Alegría, A. (2013). Iron and zinc bioavailability in Caco-2 cells: Influence of caseinophosphopeptides. *Food Chemistry, 138*(2–3), 1298–1303. https://doi.org/10.1016/j.foodchem.2012.10.113

Garner, C. M., Mills, C. O., Elias, E., & Neuberger, J. M. (1991). The effect of bile salts on human vascular endothelial cells. *BBA - Mol. Cell Res., 1091*(1), 41–45. https://doi.org/10.1016/0167-4889(91)90219-N

Gómez-Grimaldos, N. A., Gómez-Sampedro, L. J., Zapata-Montoya, J. E., López-García, G., Cilla, A., & Alegría-Torán, A. (2020). Bovine plasma hydrolysates' iron chelating capacity and its potentiating effect on ferritin synthesis in Caco-2 cells. *Food & Function, 11*(12), 10907–10912. https://doi.org/10.1039/d0fo02502j

Gonçalves, G. A., Corrêa, R. C. G., Barros, L., Dias, M. I., Calhelha, R. C., Correa, V. G., et al. (2019). Effects of *in vitro* gastrointestinal digestion and colonic fermentation on a rosemary (*Rosmarinus officinalis L*) extract rich in rosmarinic acid. *Food Chemistry, 271*, 393–400. https://doi.org/10.1016/j.foodchem.2018.07.132

Grauso, M., Lan, A., Andriamihaja, M., Bouillaud, F., & Blachier, F. (2019). Hyperosmolar environment and intestinal epithelial cells: Impact on mitochondrial oxygen consumption, proliferation, and barrier function *in vitro*. *Scientific Reports, 9*(1), 1–14. https://doi.org/10.1038/s41598-019-47851-9

International Organization for Standardization. (2009). *Biological evaluation of medical devices in Tests for in vitro cytotoxicity* (Vol. 34). Geneva: International Organization for Standardization.

Jeppsen, R., & Borzelleca, J. (1999). Safety evaluation of ferrous bisglycinate chelate. *Food and Chemical Toxicology, 37*(7), 723–731. https://doi.org/10.1016/S0278-6915(99)00052-6

Kalgaonkar, S., & Lönnerdal, B. (2009). Receptor-mediated uptake of ferritin-bound iron by human intestinal Caco-2 cells. *The Journal of Nutritional Biochemistry, 20*(4), 304–311. https://doi.org/10.1016/j.jnutbio.2008.04.003

Kitts, D. D. (2021). Antioxidant and functional activities of mrps derived from different sugar–amino acid combinations and reaction conditions. *Antioxidants, 10*(11). https://doi.org/10.3390/antiox10111840

Laparra, J. M., Glahn, R. P., & Miller, D. D. (2009). Different responses of Fe transporters in Caco-2/HT29-MTX cocultures than in independent Caco-2 cell cultures. *Cell Biology International, 33*(9), 971–977. https://doi.org/10.1016/j.cellbi.2009.06.001

Lea, T. (2015). Caco-2 cell line. In *The impact of food bioactives on health* (pp. 103–111). Springer International Publishing. https://doi.org/10.1007/978-3-319-16104-4_26.

Lin, S., Hu, X., Li, L., Yang, X., Chen, S., Wu, Y., et al. (2021). Preparation, purification and identification of iron-chelating peptides derived from tilapia (*Oreochromis niloticus*) skin collagen and characterization of the peptide-iron complexes. *Lwt, 149*(231), Article 111796. https://doi.org/10.1016/j.lwt.2021.111796

Mareček, V., Mikyška, A., Hampel, D., Čejka, P., Neuwirthová, J., Malachová, A., et al. (2017). ABTS and DPPH methods as a tool for studying antioxidant capacity of spring barley and malt. *Journal of Cereal Science, 73*, 40–45. https://doi.org/10.1016/j.jcs.2016.11.004

Neves, M. C., Filipe, H. A. L., Reis, R. L., Ramalho, J. P. P., Coreta-Gomes, F., Moreno, M. J., et al. (2019). Interaction of bile salts with lipid bilayers: An atomistic molecular dynamics study. *Frontiers in Physiology, 10*(APR), 1–11. https://doi.org/10.3389/fphys.2019.00393

Oliveira, A. S., Ferreira, C., Pereira, J. O., Pintado, M. E., & Carvalho, A. P. (2022a). Valorisation of protein-rich extracts from spent brewer's yeast (Saccharomyces cerevisiae): An overview. *Biomass Conversion and Biorefinery.* , Article 0123456789. https://doi.org/10.1007/s13399-022-02636-5

Oliveira, A. S., Ferreira, C., Pereira, J. O., Pintado, M. E., & Carvalho, A. P. (2022b). Spent brewer's yeast (Saccharomyces cerevisiae) as a potential source of bioactive peptides: An overview. *International Journal of Biological Macromolecules, 208*, 1116–1126. https://doi.org/10.1016/j.ijbiomac.2022.03.094

Oliveira, A. S., Ferreira, C. M. H., Pereira, J. O., Sousa, S., Faustino, M., Durão, J., et al. (2023). Production of iron-peptide complexes from spent yeast for nutraceutical

industry. *Food and Bioproducts Processing, 140*, 200–211. https://doi.org/10.1016/j.fbp.2023.06.006

Oliveira, C. M., Horta, B., Leal, T., Pintado, M., & Oliveira, C. S. S. (2022e). Valorization of spent sugarcane fermentation broth as a source of phenolic compounds. *Processes, 10*(7), 1339. https://doi.org/10.3390/pr10071339

Oliveira, A. S., Odila Pereira, J., Ferreira, C., Faustino, M., Durão, J., Pereira, A. M., et al. (2022c). Spent yeast valorization for food applications: Effect of different extraction methodologies. *Foods, 11*(24), 4002. https://doi.org/10.3390/foods11244002

Oliveira, A. S., Pereira, J. O., Ferreira, C., Faustino, M., Durão, J., Pintado, M. E., et al. (2022d). Peptide-rich extracts from spent yeast waste streams as a source of bioactive compounds for the nutraceutical market. *Innovative Food Science & Emerging Technologies, 81*, Article 103148. https://doi.org/10.1016/j.ifset.2022.103148

Pérez-Torres, I., Zuniga-Munoz, A., & Guarner-Lans, V. (2016). Beneficial effects of the amino acid Glycine. *Mini-Reviews in Medicinal Chemistry, 17*(1), 15–32. https://doi.org/10.2174/1389557516666160609081602

Prior, R. L., Hoang, H., Gu, L., Wu, X., Bacchiocca, M., Howard, L., et al. (2003). Assays for hydrophilic and lipophilic antioxidant capacity (oxygen radical absorbance capacity (ORACFL)) of plasma and other biological and food samples. *Journal of Agricultural and Food Chemistry, 51*(11), 3273–3279. https://doi.org/10.1021/jf0262256

Prior, R. L., Wu, X., & Schaich, K. (2005). Standardized methods for the determination of antioxidant capacity and phenolics in foods and dietary supplements. *Journal of Agricultural and Food Chemistry, 53*(10), 4290–4302. https://doi.org/10.1021/jf0502698

Remondetto, G. E., Beyssac, E., & Subirade, M. (2004). Iron availability from whey protein hydrogels: An *in vitro* study. *Journal of Agricultural and Food Chemistry, 52*(26), 8137–8143. https://doi.org/10.1021/jf040286h

Scheers, N. M., Almgren, A. B., & Sandberg, A.-S. (2014). Proposing a Caco-2/HepG2 cell model for *in vitro* iron absorption studies. *The Journal of Nutritional Biochemistry, 25*(7), 710–715. https://doi.org/10.1016/j.jnutbio.2014.02.013

Sharma, A., Shilpa Shree, B. G., Arora, S., & Kapila, S. (2017). Preparation of lactose-iron complex and its cyto-toxicity, in-vitro digestion and bioaccessibility in Caco-2 cell model system. *Food Bioscience, 20*, 125–130. https://doi.org/10.1016/j.fbio.2017.10.001

Shen, Y., Tebben, L., Chen, G., & Li, Y. (2019). Effect of amino acids on Maillard reaction product formation and total antioxidant capacity in white pan bread. *International Journal of Food Science and Technology, 54*(4), 1372–1380. https://doi.org/10.1111/ijfs.14027

Shilpashree, B. G., Arora, S., Kapila, S., & Sharma, V. (2020). Whey protein-iron or zinc complexation decreases pro-oxidant activity of iron and increases iron and zinc bioavailability. *Lebensmittel-Wissenschaft & Technologie, 126*, Article 109287. https://doi.org/10.1016/j.lwt.2020.109287

Shubham, K., Anukiruthika, T., Dutta, S., Kashyap, A. V., Moses, J. A., & Anandharamakrishnan, C. (2020). Iron deficiency anemia: A comprehensive review on iron absorption, bioavailability and emerging food fortification approaches. *Trends in Food Science & Technology, 99*, 58–75. https://doi.org/10.1016/j.tifs.2020.02.021

Sözügeçer, S., & Bayramgil, N. P. (2013). Activity of glucose oxidase immobilized onto Fe3+ attached hydroxypropyl methylcellulose films. *Colloids and Surfaces B: Biointerfaces, 101*, 19–25. https://doi.org/10.1016/j.colsurfb.2012.05.029

Suh, H., Lee, H., & Jung, J. (2003). Mycosporine Glycine protects biological systems against photodynamic damage by quenching singlet oxygen with a high efficiency. *Photochemistry and Photobiology, 78*(2), 109. https://doi.org/10.1562/0031-8655(2003)078<0109:mgpbsa>2.0.co;2

Wada, Y., & Lönnerdal, B. (2014). Bioactive peptides derived from human milk proteins - mechanisms of action. *Journal of Nutritional Biochemistry, 25*(5), 503–514. https://doi.org/10.1016/j.jnutbio.2013.10.012

Wang, X., Ai, T., Meng, X. L., Zhou, J., & Mao, X. Y. (2014). *In vitro* iron absorption of α-lactalbumin hydrolysate-iron and β-lactoglobulin hydrolysate-iron complexes. *Journal of Dairy Science, 97*(5), 2559–2566. https://doi.org/10.3168/jds.2013-7461

Wang, X., Li, M., Li, M., Mao, X., Zhou, J., & Ren, F. (2011). Preparation and characteristics of yak casein hydrolysate-iron complex. *International Journal of Food Science and Technology, 46*(8), 1705–1710. https://doi.org/10.1111/j.1365-2621.2011.02672.x

World Health Organization. (2008). *Worldwide prevalence of anaemia 1993–2005*. https://www.who.int/publications/i/item/9789241596657.

World Health Organization. (2021). *Anaemia in women and children*. Https://Www.Who.Int/Data/Gho/Data/Themes/Topics/Anaemia_in_women_and_children https://www.who.int/data/gho/data/themes/topics/anaemia_in_women_and_children. (Accessed 10 June 2021).

Wu, W., Li, B., Hou, H., Zhang, H., & Zhao, X. (2017). Identification of iron-chelating peptides from Pacific cod skin gelatin and the possible binding mode. *Journal of Functional Foods, 35*, 418–427. https://doi.org/10.1016/j.jff.2017.06.013

Wu, W., Yang, Y., Sun, N., Bao, Z., & Lin, S. (2020). Food protein-derived iron-chelating peptides: The binding mode and promotive effects of iron bioavailability. *Food Research International, 131*(1), Article 108976. https://doi.org/10.1016/j.foodres.2020.108976

Xiao, C., Toldrá, F., Zhao, M., Zhou, F., Luo, D., Jia, R., et al. (2022). *In vitro* and *in silico* analysis of potential antioxidant peptides obtained from chicken hydrolysate produced using Alcalase. *Food Research International, 157*. https://doi.org/10.1016/j.foodres.2022.111253

Zhang, Y., Ding, X., & Li, M. (2021). Preparation, characterization and *in vitro* stability of iron-chelating peptides from mung beans. *Food Chemistry, 349*(December 2020), Article 129101. https://doi.org/10.1016/j.foodchem.2021.129101